The asymmetric segregation of damaged proteins is stem cell–type dependent

Mary Rose Bufalino,[1] Brian DeVeale,[2] and Derek van der Kooy[1,2]

[1]Department of Medical Biophysics and [2]Department of Molecular Genetics, University of Toronto, Toronto, Ontario M5S 3E1, Canada

Asymmetric segregation of damaged proteins (DPs) during mitosis has been linked in yeast and bacteria to the protection of one cell from aging. Recent evidence suggests that stem cells may use a similar mechanism; however, to date there is no in vivo evidence demonstrating this effect in healthy adult stem cells. We report that stem cells in larval (neuroblast) and adult (female germline and intestinal stem cell) *Drosophila melanogaster* asymmetrically segregate DPs, such as proteins with the difficult-to-degrade and age-associated 2,4-hydroxynonenal (HNE) modification. Surprisingly, of the cells analyzed only the intestinal stem cell protects itself by segregating HNE to differentiating progeny, whereas the neuroblast and germline stem cells retain HNE during division. This led us to suggest that chronological life span, and not cell type, determines the amount of DPs a cell receives during division. Furthermore, we reveal a role for both niche-dependent and -independent mechanisms of asymmetric DP division.

Introduction

Aging at the cellular level is generally characterized by a decline in cell function and has been correlated with the accumulation of cellular components, such as proteins, damaged by reactive oxygen species (ROS; Giorgio et al., 2007). Despite the recent focus on the impact of aging stem cells on organism health, no studies have addressed whether adult stem cells are capable of resetting their age by directing damaged proteins (DPs) to differentiating progeny.

So far, the most well studied systems of the asymmetric segregation of damage, which include ROS-damaged DNA, proteins, and lipids, are in bacteria and yeast (Aguilaniu et al., 2003; Lindner et al., 2008; Shcheprova et al., 2008). Protein aggregates in *Escherichia coli* accumulate in the old pole of the cell with age and are associated with a decreased growth rate (Lindner et al., 2008). In yeast, carbonylated proteins and extrachromosomal ribosomal DNA circles are retained by the mother cell during asymmetric division, whereas the daughter bud cell is rejuvenated (Aguilaniu et al., 2003; Shcheprova et al., 2008). This unequal partitioning of DPs during mitosis appears to be a well-conserved phenomenon, also found for proteins destined for degradation in human embryonic and mammalian fibroblast cell lines (Fuentealba et al., 2008). Furthermore, huntingtin is polarized during division when it is expressed in human embryonic and mammalian somatic cell lines and embryonic *Drosophila melanogaster* neuroblasts (NBs; Rujano et al., 2006).

To determine if the asymmetrical segregation of DPs is conserved in a nondiseased state in vivo, we probed for proteins directly modified on a histidine residue by an endogenous marker of DPs, 2,4-hydroxynonenal (HNE). HNE is a product of lipid peroxidation that is highly reactive and readily forms covalent bonds with proteins that have been oxidized, making them resistant to proteolysis through the proteasome, although they are susceptible to lysosomal degradation (Friguet and Szweda, 1997; Marques et al., 2004). HNE has previously been identified as an indicator of oxidative stress and contains carbonyl groups, which increase with age and can affect the catalytic activity of proteins. It also identifies a wider range of proteins containing modifications associated with oxidative stress compared to alternative methods (Toroser et al., 2007). Furthermore, increased levels of lipid peroxidation products are common to many neurodegenerative diseases (Butterfield et al., 2011).

Using HNE as an indicator of DPs, we assessed its asymmetric segregation in the female germline stem cell (GSC),

Correspondence to Mary Rose Bufalino: maryrose.bufalino@utoronto.ca

Abbreviations used in this paper: ANOVA, analysis of variance; CB, cystoblast; DCAD, DE-Cadherin; DP, damaged protein; EB, enteroblast; GMC, ganglion mother cell; GSC, germline stem cell; HNE, 2,4-hydroxynonenal; ISC, intestinal stem cell; NB, neuroblast; ROS, reactive oxygen species; UP, ubiquitinated protein.
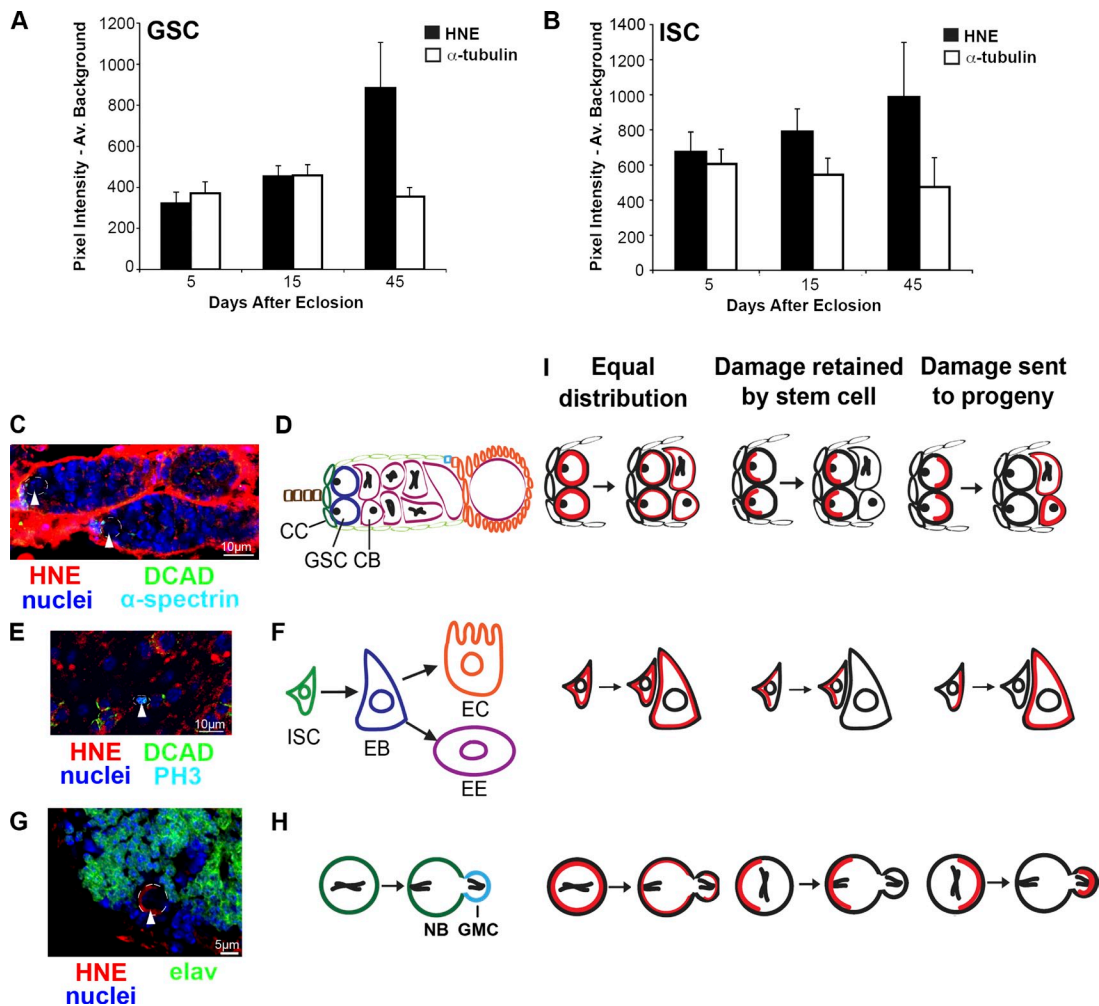
Figure 1. **GSCs accumulate more HNE with age compared with ISCs, indicating separate modes of HNE distribution during mitosis.** (A) GSCs accumulate HNE during aging (n = 10 for each time point). (B) Contrary to the GSC, HNE does not accumulate significantly with age in ISCs (n ≥ 10 for each time point). (C and D) Each germarium contains GSCs (arrowheads), which reside adjacent to cap cells (CC) and divide asymmetrically to give rise to CBs. An enlarged image of one of the germaria in C is shown in Fig. S1 I. (E and F) ISCs (arrowhead) self-renew and produce an EB, which can differentiate into an enterocyte (EC) or enteroendocrine cell (EE). (G and H) NBs (arrowhead) divide asymmetrically to self-renew and produce a GMC, which generally divides to give rise to neurons. (I) Potential types of DP (red) segregation are shown in the GSC (top), ISC (middle), and NB (bottom). The mean (±SEM) represents HNE (or alternative stain) pixel intensity subtracted by average background.

adult intestinal stem cell (ISC), and larval NBs of *Drosophila*. Each ovary is made up of ~20 ovarioles, each containing one germarium. Two to three GSCs are anchored to cap cells, which maintain the stem cells by secreting bone morphogenetic protein that suppresses transcription of a differentiation gene, *bag-of-marbles* (Fuller and Spradling, 2007). Through asymmetric division, GSCs self-renew and create a cystoblast (CB) that goes through four rounds of division with incomplete cytokinesis to finally generate a 16-cell cyst (Kirilly and Xie, 2007; Fig. 1, C and D). ISCs replace the differentiated cells of the posterior midgut approximately every week. ISCs self-renew and produce an enteroblast (EB), which differentiates into either an enterocyte or enteroendocrine cell (Micchelli and Perrimon, 2006; Ohlstein and Spradling, 2006; Fig. 1, E and F). NBs divide asymmetrically to self-renew and produce a ganglion mother cell (GMC), which then generally divides symmetrically to create the neurons of the adult brain (Fig. 1, G and H).

Results and discussion

HNE is a marker of DPs that accumulate with oxidative stress and age

To validate HNE as a marker for DPs, GSCs were assessed after exposure to oxidative stress and aging. Flies (10 d after eclosion) were treated for 24 h with either a xenobiotic that induces ROS production upon ingestion (10 mM paraquat) in 5% sucrose or 5% sucrose alone at 25°C. GSCs have greater (threefold) HNE staining in paraquat-treated compared with sucrose-treated flies (P < 0.05; Fig. S1, E–G). HNE has been found to accumulate with age in *Drosophila* flight muscles (Toroser et al., 2007) and through the modification of proteins contributes to general cell dysfunction associated with aging (e.g., HNE disrupts DNA synthesis, protein production, enzyme function, and the ability of cells to communicate through gap junctions; Okada et al., 1999). Ovaries stained for HNE and α-tubulin as a control revealed that mean HNE
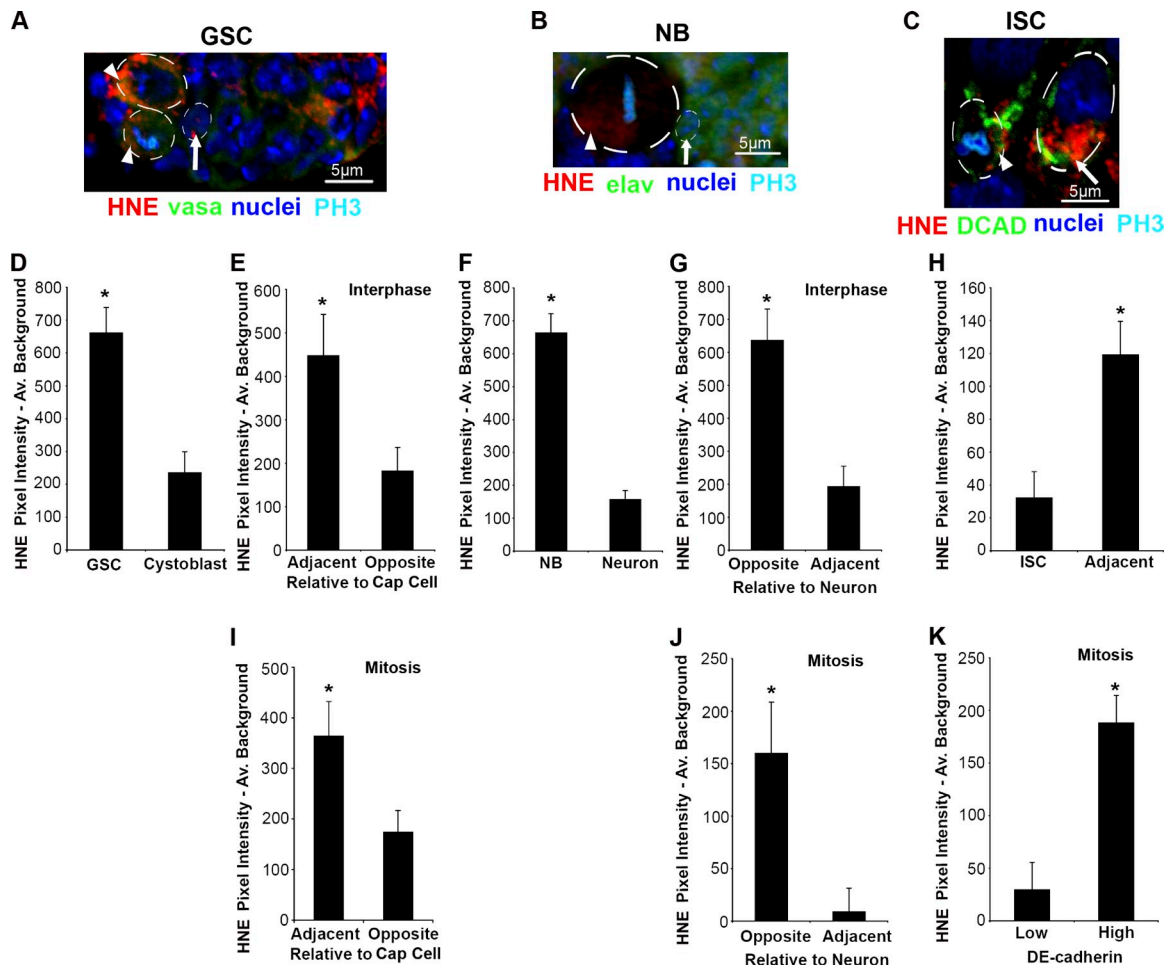
Figure 2. **HNE is asymmetrically distributed in the GSC, NB, and ISC.** (A) Example of a germarium containing GSCs (arrowheads) and adjacent CB (arrow). Individual color channels are shown for the same image in Fig. S2 A. (B) Example of a NB (arrowhead) with polarized HNE that contains greater HNE content than adjacent neurons (arrow). Individual color channels are shown for the same image in Fig. S2 B. (C) Example of an ISC (arrowhead) with an asymmetric distribution of HNE and adjacent differentiated cell (arrow). Individual color channels are shown for the same image in Fig. S2 C. (D) GSCs contain significantly more damage (HNE) than adjacent cells (CBs or cystocytes; $n = 11$), and during interphase HNE is localized to the site opposite of CB production (E; $n = 11$; 11/11 cells asymmetric). (F) Similar to the GSC, the NB contains more HNE than adjacent progeny ($n = 16$), and during interphase HNE is localized to the site opposite of new neurons (G; $n = 10$; 9/10 cells asymmetric). (H) In contrast, ISCs contain less damage than adjacent differentiated cells ($n = 10$). During mitosis, HNE asymmetry is maintained in the GSC (I; $n = 8$; 6/8 cells asymmetric) and NB (J; $n = 12$; 11/12 cells asymmetric). (K) ISCs also have polarized HNE during mitosis, when the cell is separated based on DCAD staining intensity ($n = 10$; 10/10 cells asymmetric). The mean (±SEM) represents HNE pixel intensity subtracted by average background. *, $P < 0.05$ by paired two-tailed t test.

intensity increases significantly with age in GSCs (Fig. 1 A and Fig. S1 C; $P < 0.05$ by one-way analysis of variance [ANOVA]), with a 2.75-fold increase between 5 and 45 d. Therefore, HNE represents a protein modification associated with oxidative stress and age. Unexpectedly, ISCs did not display a significant increase in HNE with age when identified as small cells in mitosis (Fig. 1 B and Fig. S1 D; $n \geq 10$ for each time point; $P > 0.05$ by one-way ANOVA) and as the smallest cell in a BrdU[+] lineage (Fig. S1 B; $n \geq 8$ for each time point; $P > 0.05$ by one-way ANOVA). This unexpected difference in the extent of HNE accumulation with age between GSCs and ISCs prompted us to look at other differences in stem cell populations with respect to HNE.

Stem cells and progeny differ in HNE levels
HNE-modified proteins in GSCs, NBs, and ISCs may be uniformly distributed within stem cells or polarized to one end of

the cell, leading to their asymmetric segregation during mitosis (Fig. 1 I). Based on the accumulation of HNE in GSCs with age, it was predicted that GSCs but not ISCs retain DPs at division. As a result of polarized HNE, stem cells and adjacent progeny should differ in HNE levels. GSCs exceed adjacent progeny (2.8-fold) in mean cytoplasmic HNE intensity ($P < 0.05$, paired two-tailed t tests; Fig. 2, A and D; and with channels separated in Fig. S2 A). This trend is conserved during aging; GSCs have significantly more HNE than CBs at each time point ($P < 0.05$, paired two-tailed t tests; Fig. S1 A) and HNE content in CBs does not significantly increase with age ($P > 0.05$, one-way ANOVA; Fig. S1, A and C). Similar to GSCs, NBs have greater (4.27-fold) mean cytoplasmic HNE intensity than adjacent neurons ($P < 0.05$; Fig. 2, B and F). In contrast, there is significantly reduced (3.73-fold) mean HNE staining in ISCs compared with adjacent progeny ($P < 0.05$; Fig. 2, C and H). This trend is conserved during aging;
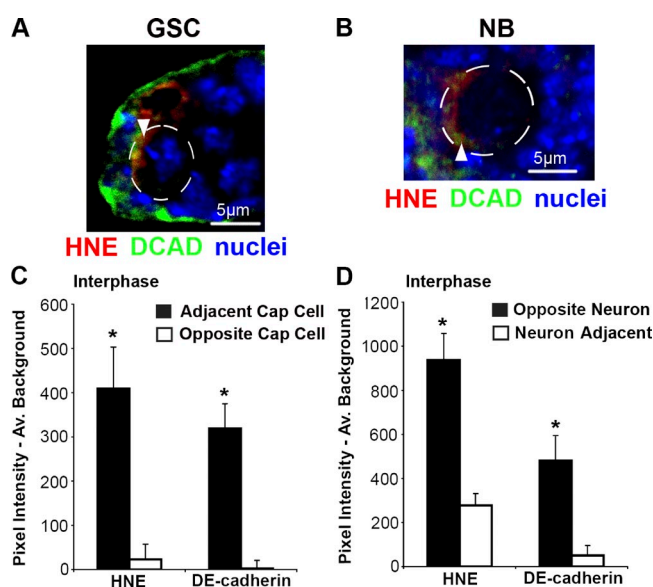
A GSC

B NB

HNE DCAD nuclei (A)

HNE DCAD nuclei (B)

C Interphase

■ Adjacent Cap Cell
□ Opposite Cap Cell

Pixel Intensity - Av. Background

HNE   DE-cadherin

D Interphase

■ Opposite Neuron
□ Neuron Adjacent

Pixel Intensity - Av. Background

HNE   DE-cadherin

Figure 3. **DCAD and HNE colocalize.** Examples of regions of intense DCAD staining that colocalize with areas of high HNE staining (arrowhead) in the GSC (A) and NB (B). Similar to ISCs (Fig. 2 K), within GSCs (C; n = 11; 10/11 cells asymmetric) and NBs (D; n = 9; 9/9 cells asymmetric) there is significantly more HNE and DCAD at the side of the cell opposite to new differentiating progeny during interphase. The mean (±SEM) represents HNE (or alternative stain) pixel intensity subtracted by average background. *, P < 0.05 by paired two-tailed *t* test.

ISCs (identified as the smallest BrdU-positive cell in a BrdU-positive cell cluster) have significantly less HNE than adjacent EBs at each time point (P ≤ 0.05, paired two-tailed *t* tests; Fig. S1 B). To confirm that EBs contain more HNE than ISCs, EBs were identified as β-galactosidase–positive cells in Gbe+Su(H)lacZ flies (Furriols and Bray, 2001) and found to contain 1.54-fold greater HNE than adjacent small β-galactosidase–negative cells (P < 0.05; Fig. S1, R and S).

Intracellular HNE distributes asymmetrically
In support of asymmetric segregation, each stem cell type contains polarized HNE staining. GSCs contain significantly more HNE in the region adjacent to cap cells during interphase (2.47-fold; P < 0.05; Fig. 2 E) and mitosis (2.1-fold; P < 0.05; Fig. 2 I). This result was confirmed using a second HNE antibody, which has 1.97-fold greater HNE on the cap cell side of the GSC during interphase (P < 0.05; Fig. S1, H and I). Similar to GSCs, NBs contain greater HNE staining in the area farthest from adjacent progeny during interphase (3.32-fold; P < 0.05; Fig. 2 G) and mitosis (19.2-fold; P < 0.05; Fig. 2 J). Regions of high DE-Cadherin (DCAD) staining were used to predict the side of an ISC that would form the EB; the point of contact between ISCs and EBs is rich in β-catenin and DCAD (Maeda et al., 2008). In ISCs, greater HNE staining (6.49-fold) is found in regions of high DCAD expression during mitosis (P < 0.05; Fig. 2 K). Therefore, HNE is localized to the side of the ISC most likely to contribute to the EB. Ubiquitinated proteins (UPs) are marked for degradation through the proteasome and, similar to HNE, are detected in neurodegenerative diseases (Vernace et al., 2007). The same trend of intracellular accumulation identified for HNE was found for UPs in the GSC (1.58-fold; P < 0.05; Fig. S1, J and M), NB

(1.24-fold; P < 0.05; Fig. S1, K and N), and ISC (1.5-fold; P < 0.05; Fig. S1, L and O). UPs also colocalize with a NB polarity protein, PKCϛ, to the side opposite of GMC production with 1.87-fold greater UP staining during mitosis (P < 0.05; Fig. S1, P and Q). This suggests that asymmetric segregation exists for DPs with different modifications.

Based on the intracellular localization data we suggest that chronological life span, and not cell type, determines the amount of DPs a cell receives during division. The GSC is shorter lived than its CB progeny because the CB can form a new organism with the ability to outlive the mother where the GSC resides. Similarly, the NB undergoes apoptosis or differentiates into unknown cell types during pupation, making it shorter lived than its neuronal progeny, which persist to adulthood (Chell and Brand, 2008). Therefore GSCs and NBs protect their longer-lived differentiating progeny by retaining a factor associated with aging. This is distinct from ISCs, present throughout the organisms' life span, that segregate HNE toward differentiating progeny, which are replaced approximately every week (Micchelli and Perrimon, 2006; Ohlstein and Spradling, 2006).

In each stem cell population HNE associates with a niche adhesion molecule
DCAD has important roles in the niche of all three stem cell systems (Song et al., 2002; Dumstrei et al., 2003; Maeda et al., 2008) and is involved in the asymmetric division of *Drosophila* male GSCs through its effects on spindle orientation (Inaba et al., 2010). GSCs in interphase contain greater DCAD (122.8-fold) and HNE (17.7-fold) adjacent to cap cells (P < 0.05 for both; Fig. 3, A and C). Within NBs in interphase, more DCAD (9.5-fold) and HNE (3.38-fold) are found opposite neuron production (P < 0.05 for both; Fig. 3, B and D). Therefore, despite the differences in DP distribution with respect to differentiating progeny, HNE and DCAD colocalize in all three stem cell populations.

GSCs displaced from their niche lose some but not all HNE polarization
The progeny of GSCs require the expression of a differentiation-promoting gene, *bam*, to differentiate, and in its absence the germarium is filled with undifferentiated GSC-like cells. A deletion mutant, *bam*$^{\Delta 86}$ (McKearin and Ohlstein, 1995), was used to determine the effect of contact with stem cell niche cells on the localization of HNE within stem cells. *bam*$^{\Delta 86}$/*bam*$^{\Delta 86}$ flies maintained at 25°C for 20 d displayed an accumulation of undifferentiated cells with a spectrosome, an organelle rich in membrane skeleton proteins that anchors the mitotic spindle (Deng and Lin, 1997), indicated by α-spectrin staining (Fig. 4 A; and channels separated in Fig. S3 A). Undifferentiated cells in interphase within the GSC niche with high DCAD content contain 1.71-fold greater HNE adjacent to cap cells (P < 0.05; Fig. 4, A and B; and Fig S3 A). Undifferentiated cells at least two cells away from the GSC niche also displayed polarized HNE during interphase; however, not to the same extent as those cells within the niche. These cells contained 1.42-fold greater HNE at the side of the cell with the spectrosome (P < 0.05; Fig. 4, A and C; and Fig. S3 A).

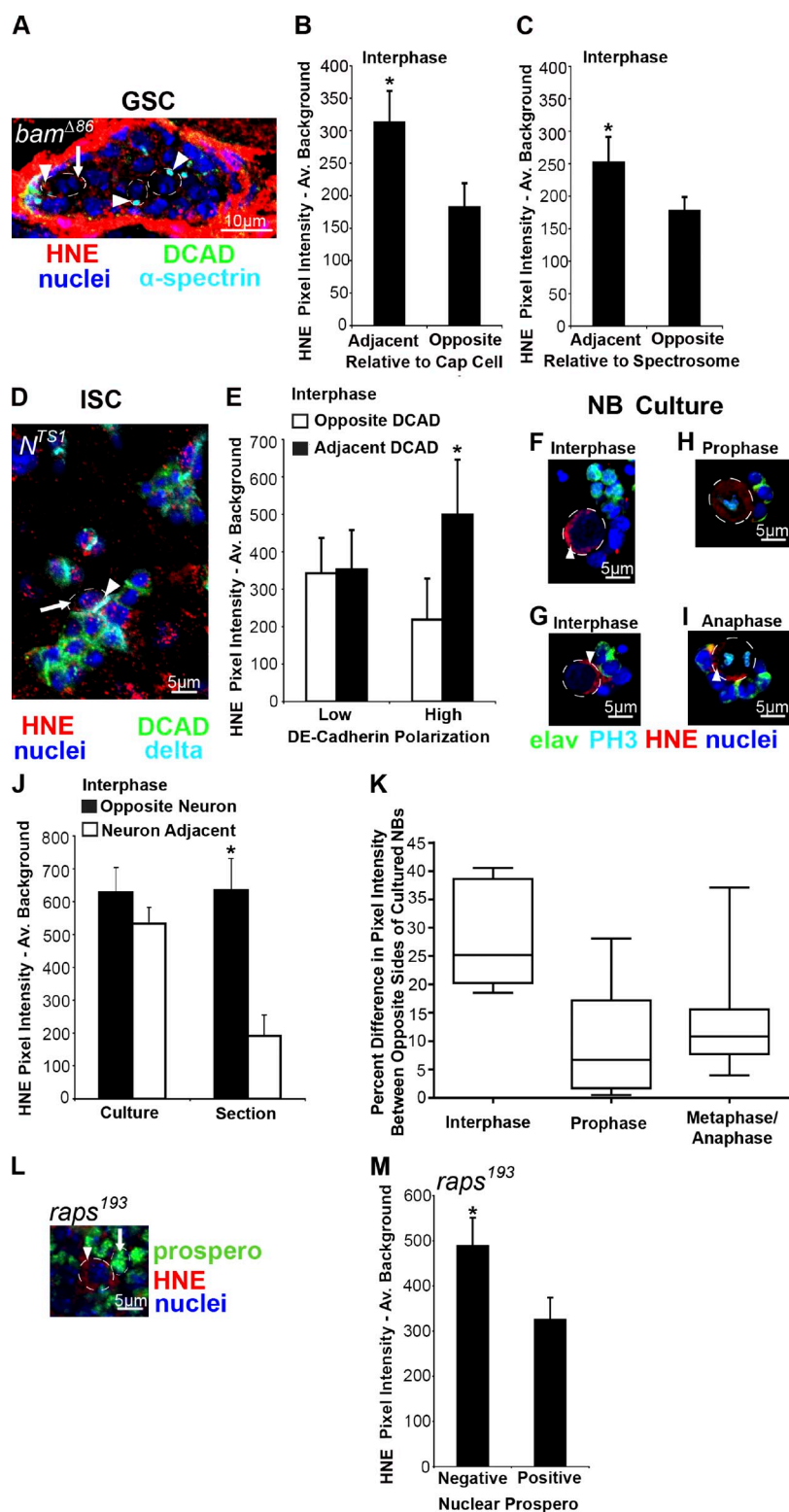**Figure 4. The niche is involved in HNE asymmetry.** (A) Example of a $bam^{\Delta 86}/bam^{\Delta 86}$ germarium where GSC-like cells contain polarized HNE in both cells adjacent to the stem cell niche (leftmost arrowhead indicates region adjacent to cap cells and arrow indicates opposite region) and at least two cells removed from the niche (arrowheads). Individual color channels are shown for the same image in Fig. S3 A. (B) HNE remains localized to the anterior end of cells in interphase within the GSC niche in $bam^{\Delta 86}/bam^{\Delta 86}$ germariums ($n = 12$; 12/12 cells asymmetric). (C) Cells in $bam^{\Delta 86}/bam^{\Delta 86}$ germariums, which have intense HNE staining and are at least two cells away from the niche, also display polarized HNE during interphase that localizes to the spectrosome ($n = 10$; 6/10 cells asymmetric). (D) Examples of delta-positive clusters of ISC-like cells within a N^{ts1}/N^{ts1} midgut. Arrowhead indicates region of intense DCAD staining that colocalizes with the most intense region of HNE staining compared with opposite side (arrow). Individual color channels are shown for the same image in Fig. S3 B. (E) Only cells within delta-positive N^{ts1}/N^{ts1} cell clusters with a high level of DCAD polarization contain an asymmetric distribution of HNE during interphase ($n = 9$; 9/9 cells asymmetric). Cells with low (2× less) DCAD polarization do not have an asymmetric distribution of HNE during interphase ($n = 7$; 1/7 cells asymmetric). (F and G) Examples of cultured NBs (circled) in interphase; HNE does not consistently localize to the side of the cell opposite neurons. (J) Asymmetric HNE localization to the side of NBs opposite adjacent neurons is lost when the NB niche is disrupted during cell culture ($n = 8$; 1/8 cells asymmetric). (K) The polarization of HNE increases in mitotic cells with cell cycle progression (prophase example in H, $n = 15$; metaphase and anaphase example in I, $n = 17$; interphase, $n = 8$). (M) Symmetrically dividing NBs in $raps^{193}/raps^{193}$ mutants (L, arrowhead) identified as Prospero-negative cells contain greater HNE staining than adjacent cells (arrow) of a similar size during interphase ($n = 9$). The mean (±SEM) represents HNE pixel intensity subtracted by average background. *, $P < 0.05$ by paired two-tailed t test.

The spectrosome is associated with the centrosome (Lin et al., 1994); therefore, the centrosome may be involved in DP polarization. Accumulated misfolded proteins actively localize to the aggresome, a structure associated with the spindle-pole body in yeast (Wang et al., 2009) and centrosome in *Drosophila* and mammals (Rujano et al., 2006). Still, the extent of HNE polarization was greatest in cells within the niche, suggesting that baseline levels of HNE do not depend exclusively on centrosome association for their asymmetric distribution.

The extent of DCAD polarization predicts HNE asymmetry in ISCs

The fate of ISC progeny depends on Notch signaling, with high levels of Delta leading to EB and low levels to enteroendocrine

cell production (Ohlstein and Spradling, 2007). To assess the effect of niche disruption on the asymmetrical distribution of DPs in ISCs, we used a temperature-sensitive Notch mutant (N^{ts1}; Shellenbarger and Mohler, 1975), which produces clusters of delta-positive ISC-like cells when cultured at 29°C for 10 d (Fig. 4 D and channels separated in Fig. S3 B). HNE remains localized to DCAD within ISC-like cells in interphase. Cells within clusters were separated into low and high DCAD polarization (two times greater polarity than low condition). In low DCAD polarity cells, no significant polarization of HNE is found (P > 0.05; Fig. 4 E), and in high DCAD polarity cells HNE remains localized (2.28-fold) to regions of intense DCAD during interphase (P < 0.05; Fig. 4, D and E). Therefore, when an ISC-like cell is in an environment similar to the stem cell niche (high DCAD polarization) DP localization is preserved.

Both niche-dependent and -independent factors are responsible for HNE polarization in NBs

When NBs are mechanically dissociated they can be separated from their niche in culture. Within 20 min of being in culture, NBs in interphase with no cell–cell contact or only in contact with a small cluster of neurons show no significant asymmetric localization of HNE to the side of the NB opposite neurons (P > 0.05; Fig. 4, F and G). Surprisingly, HNE becomes increasingly localized to one region of mitotic NBs as the cell cycle progresses; more NBs in metaphase and anaphase contain a greater difference in HNE staining between two sides of the cell than those in prophase (P < 0.05 by χ^2 test; Fig. 4, H, I, and K). This finding supports the existence of a niche-independent mechanism of DP segregation, such as the polarisome. In yeast, the polarisome is responsible for retrograde transport of protein aggregates along actin cables from the bud to the mother during cell division (Liu et al., 2010) and a similar mechanism may be conserved in *Drosophila*. Interestingly, the extent of HNE polarization in mitotic NBs in culture does not reach that of cultured NBs in interphase (13 vs. 28%), if the cell is divided based on pixel intensity instead of neuron position (Fig. 4 K). This finding suggests that the plane of polarization may be reset during mitosis and that the niche is needed to reach the maximum level of polarization.

Alternatively, DPs may accumulate in NBs because they are larger than daughter GMCs or because they are associated with the mitotic spindle, like many polarity proteins in the NB. We explored these possibilities using a mutant of Rapsynoid/Partner of Inscuteable (Raps), a cortical polarity protein in the NB responsible for spindle orientation and size of daughter cells (Siller et al., 2006). In the $raps^{193}/raps^{193}$ mutant the large size difference between NBs and GMCs and the asymmetric distribution of proteins normally localized to the NB (Inscuteable) and GMC (Miranda) are disrupted (Parmentier et al., 2000). However, NBs can be distinguished from GMCs by their absence of nuclear Prospero. We found that $raps^{193}/raps^{193}$ mutant NBs in interphase contain significantly greater HNE content (1.50-fold) than adjacent progeny (P < 0.05; Fig. 4, L and M). On average, the Prospero-negative cells were only 1.9%

larger than adjacent Prospero-positive cells; therefore, DPs do not accumulate in NBs because of their large size or association with the mitotic spindle and future studies should examine other mechanisms of asymmetric distribution, such as the polarisome.

Conclusions

DPs are polarized in GSCs, NBs, and ISCs and inherited by the cell with the shortest functional life span (GSC, NB, and EB), which may defend against one cause of aging, the build-up of molecules damaged by ROS (Giorgio et al., 2007). As a result of the deleterious effects caused by a build-up of DPs, multiple mechanisms may exist to ensure their proper segregation. We found that the stem cell niche plays a role in this asymmetry, but is not the only mechanism of DP segregation. We suggest that both the stem cell niche and niche-independent mechanisms are responsible for the asymmetric segregation of DPs.

Materials and methods

Flies

Wild-type Oregon R flies (U. Tepass, University of Toronto, Toronto, Canada) were raised on standard cornmeal/sugar/yeast/agar diet at 25°C with 50% relative humidity on a 12-h light–dark cycle. $bam^{\Delta86}$ (Bloomington Stock Center, Indiana University) and $raps^{193}$ (Bloomington Stock Center) flies were maintained in the same conditions as wild type. N^{TS1} flies (Bloomington Stock Center) were maintained at 21°C and moved to 29°C for 10 d during experiments.

Immunohistochemistry

All tissues were dissected in Schneider's Drosophila medium, rinsed with PBS, fixed for 20 min in Bouin's fixative, and washed for 20 min in 70% ethanol. Ovaries and larval brains were sectioned at 6 and 10 µm, respectively, before staining. Blocking was performed for 1 h at RT in 5% normal goat serum solution of PBS with 0.2% Triton X-100. Tissue was incubated in primary antibodies at 4°C overnight in PBS/1% normal goat serum/0.2% Triton X-100 and after three washes (PBS/0.2% Triton X-100) in secondary antibodies for 2 h at RT in PBS/1% normal goat serum/0.2% Triton X-100. Alternatively, ovaries in the aging experiment were stained as whole mounts after10-min incubation in a 0.05% trypsin solution with 1% calcium chloride at 37°C, with incubation in primary and secondary antibodies increased to two nights on a shaker. To stain membranes, 2.5 µg/ml Fast Dil (Invitrogen) was applied to tissues for 1 h at 4°C after trypsin treatment and tissues were permeabilized with 0.3% Tween 20 in PBS for 2 h at 4°C before immunohistochemistry. To stain intestines, the entire gastrointestinal tract was dissected and then stained as previously described for larval brain and ovary tissue with the exception that tissue was not sectioned, blocking was increased to 3 h at 4°C, and primary antibodies were washed for 2 h at 4°C before incubation with secondary antibodies for 3 h at 4°C. The following primary antibodies were used with appropriate Alexa-conjugated secondary antibodies (1:300) followed by Hoescht 33258 (1:1,000; Sigma-Aldrich) for 10 min at RT: 20 µg/ml mouse anti-HNE (R&D Systems), rabbit anti-HNE (1:50; Abcam), rabbit anti–Histone H3 (1:100; Abcam), rat anti-Elav (1:10; Developmental Studies Hybridoma Bank [DSHB]), mouse anti–α-spectrin (1:20; DSHB), mouse anti-delta (1:10; DSHB), mouse anti-Prospero (1:10; DSHB), rat anti-DCAD (gut and ovary; 1:20; DSHB), rat anti-DCAD (larval brain; 1:500; a gift from V. Hartenstein, University of California, Los Angeles, Los Angeles, CA), and rat anti-Vasa (1:4; DSHB). All samples were mounted in an aqueous mounting medium (Fluoro-Gel; Electron Microscopy Sciences). Images were captured at RT with a 12.8-megapixel cooled digital color camera (DP72; Olympus) using the 60× (NA 0.85) water immersion objective of a confocal laser scanning microscope (FV1000, Olympus). The following fluorochromes were used: Alexa Fluor 405, 488, 568, and 647. Brightness and contrast of entire images were adjusted with FV1000 software.

NB cell culture

Brains were removed from L3 larvae and immediately placed in Schneider's Drosophila medium supplemented with 5% fetal bovine serum.

The ventral nerve cord was removed and the central brain and optic lobe were mechanically dissociated using the tips of 30 1/2-gauge needles, in poly-D-lysine–coated coverslip bottom dishes (MatTek Corporation). After allowing cells to adhere to the dish for 20 min at 25°C in the dark they were rinsed with PBS before fixing for 20 min and staining exactly as larval brain slices with the exception that cells were counterstained with 2× Hoescht 33258.

Image analysis

ImageJ was used to analyze all images. ISCs were identified as small cells in mitosis unless otherwise noted. $raps^{193}/raps^{193}$ mutant NBs were identified as nuclear Prospero-negative cells that were no more than 15% larger than adjacent Prospero-positive cells. All staining intensity measurements are presented as pixel intensity subtracted by average background. Average cytoplasmic staining, used to compare stem cells and adjacent progeny, was measured by drawing boundaries around the nucleus as identified by Hoescht staining. Average background was calculated by averaging areas of minimal pixel intensity within the tissue being analyzed or the cell culture plate. The distribution of staining within a cell was calculated by generating a plot profile for each cell and then averaging the pixel intensity contained in opposite ends of the cell. Each end was separated by the nucleus, which contained minimal staining and was standardized as the center 30% of the GSC and ISC and 60% of the NB.

Statistical analysis

Paired two-tailed t tests were used to analyze localization measurements and compare adjacent cells and a one-way ANOVA was used to determine the effect of age on staining. A χ^2 test was used to determine if the frequency of NBs with different amounts of HNE asymmetry varied between cells in prophase and metaphase/anaphase. Results were considered statistically significant when $P < 0.05$. All statistical tests were completed using Prism 4 (GraphPad Software). A cell was classified as asymmetric if HNE content was ≥35% greater on the side of the cell predicted to have greater staining or UP content was ≥20% greater.

Supplemental materials and methods

For the comparison of ISCs and adjacent EBs during aging, flies were transferred to medium (5% sucrose, 5% yeast extract, and 0.5% agarose) that contained 0.2 mg/ml BrdU 4 d before the aging time point (sheep anti-BrdU was used at 1:50; Invitrogen). Paraquat (methyl viologen dichloride hydrate) was obtained from Sigma-Aldrich. Gbe⁺Su(H)LacZ flies (a gift from B. Ohlstein, Columbia University, New York, NY; Furriols and Bray, 2001) were maintained in the same conditions as wild type and chicken anti–β-galactosidase was used at 1:1,000 (Abcam). To identify poly-UPs, mouse anti-polyubiquitin (1:100; Enzo Life Sciences) was used. NBs stained weakly for mouse anti-polyubiquitin; however, an antibody reactive to both mono- and poly-UPs (1:100; Enzo Life Sciences) that has been shown to increase with age in flies (Demontis and Perrimon, 2010) was above the detection limit and was used. Rabbit anti-PKCζ was used at 1:1,000 (C20; Santa Cruz Biotechnology, Inc.).

Online supplemental material

The asymmetric segregation of DPs within all three stem cell populations is supported by the data in Fig. S1. This includes a comparison of the levels of DPs within GSCs and ISCs with their adjacent progeny. To validate the markers of DPs, the levels of HNE found within GSCs when the whole organism is exposed to oxidative stress are compared, and the distribution of a second HNE antibody and antibodies labeling UPs are shown within each stem cell population. NBs are further identified by PKCζ staining and the localization of DPs relative to PKCζ is described. To further identify ISC progeny, the DP content of LacZ-positive cells from Gbe⁺Su(H)LacZ flies are compared with adjacent small cells. Fig. S2 displays each channel separated for the mitotic GSC, NB, and ISC images shown in Fig. 2 (A–C) and the method of DP localization measurements. Fig. S3 displays each channel separated for the images of a $bam^{\Delta86}/bam^{\Delta86}$ germarium and N^{ts1}/N^{ts1} midgut shown in Fig. 4 (A and D). Online supplemental material is available at http://www.jcb.org/cgi/content/full/jcb.201207052/DC1.

References

Aguilaniu, H., L. Gustafsson, M. Rigoulet, and T. Nyström. 2003. Asymmetric inheritance of oxidatively damaged proteins during cytokinesis. *Science*. 299:1751–1753. http://dx.doi.org/10.1126/science.1080418

Butterfield, D.A., T. Reed, and R. Sultana. 2011. Roles of 3-nitrotyrosine- and 4-hydroxynonenal-modified brain proteins in the progression and pathogenesis of Alzheimer's disease. *Free Radic. Res.* 45:59–72. http://dx.doi.org/10.3109/10715762.2010.520014

Chell, J.M., and A.H. Brand. 2008. Forever young: death-defying neuroblasts. *Cell*. 133:769–771. http://dx.doi.org/10.1016/j.cell.2008.05.010

Demontis, F., and N. Perrimon. 2010. FOXO/4E-BP signaling in *Drosophila* muscles regulates organism-wide proteostasis during aging. *Cell*. 143:813–825. http://dx.doi.org/10.1016/j.cell.2010.10.007

Deng, W., and H. Lin. 1997. Spectrosomes and fusomes anchor mitotic spindles during asymmetric germ cell divisions and facilitate the formation of a polarized microtubule array for oocyte specification in *Drosophila*. *Dev. Biol.* 189:79–94. http://dx.doi.org/10.1006/dbio.1997.8669

Dumstrei, K., F. Wang, and V. Hartenstein. 2003. Role of DE-cadherin in neuroblast proliferation, neural morphogenesis, and axon tract formation in *Drosophila* larval brain development. *J. Neurosci.* 23:3325–3335.

Friguet, B., and L.I. Szweda. 1997. Inhibition of the multicatalytic proteinase (proteasome) by 4-hydroxy-2-nonenal cross-linked protein. *FEBS Lett.* 405:21–25. http://dx.doi.org/10.1016/S0014-5793(97)00148-8

Fuentealba, L.C., E. Eivers, D. Geissert, V. Taelman, and E.M. De Robertis. 2008. Asymmetric mitosis: unequal segregation of proteins destined for degradation. *Proc. Natl. Acad. Sci. USA*. 105:7732–7737. http://dx.doi.org/10.1073/pnas.0803027105

Fuller, M.T., and A.C. Spradling. 2007. Male and female *Drosophila* germline stem cells: two versions of immortality. *Science*. 316:402–404. http://dx.doi.org/10.1126/science.1140861

Furriols, M., and S. Bray. 2001. A model Notch response element detects Suppressor of Hairless-dependent molecular switch. *Curr. Biol.* 11:60–64. http://dx.doi.org/10.1016/S0960-9822(00)00044-0

Giorgio, M., M. Trinei, E. Migliaccio, and P.G. Pelicci. 2007. Hydrogen peroxide: a metabolic by-product or a common mediator of ageing signals? *Nat. Rev. Mol. Cell Biol.* 8:722–728. http://dx.doi.org/10.1038/nrm2240

Inaba, M., H. Yuan, V. Salzmann, M.T. Fuller, and Y.M. Yamashita. 2010. E-cadherin is required for centrosome and spindle orientation in *Drosophila* male germline stem cells. *PLoS ONE*. 5:e12473. http://dx.doi.org/10.1371/journal.pone.0012473

Kirilly, D., and T. Xie. 2007. The *Drosophila* ovary: an active stem cell community. *Cell Res.* 17:15–25. http://dx.doi.org/10.1038/sj.cr.7310123

Lin, H., L. Yue, and A.C. Spradling. 1994. The *Drosophila* fusome, a germline-specific organelle, contains membrane skeletal proteins and functions in cyst formation. *Development*. 120:947–956.

Lindner, A.B., R. Madden, A. Demarez, E.J. Stewart, and F. Taddei. 2008. Asymmetric segregation of protein aggregates is associated with cellular aging and rejuvenation. *Proc. Natl. Acad. Sci. USA*. 105:3076–3081. http://dx.doi.org/10.1073/pnas.0708931105

Liu, B., L. Larsson, A. Caballero, X. Hao, D. Oling, J. Grantham, and T. Nyström. 2010. The polarisome is required for segregation and retrograde transport of protein aggregates. *Cell*. 140:257–267. http://dx.doi.org/10.1016/j.cell.2009.12.031

Maeda, K., M. Takemura, M. Umemori, and T. Adachi-Yamada. 2008. E-cadherin prolongs the moment for interaction between intestinal stem cell and its progenitor cell to ensure Notch signaling in adult *Drosophila* midgut. *Genes Cells*. 13:1219–1227. http://dx.doi.org/10.1111/j.1365-2443.2008.01239.x

Marques, C., P. Pereira, A. Taylor, J.N. Liang, V.N. Reddy, L.I. Szweda, and F. Shang. 2004. Ubiquitin-dependent lysosomal degradation of the HNE-modified proteins in lens epithelial cells. *FASEB J.* 18:1424–1426.

McKearin, D., and B. Ohlstein. 1995. A role for the *Drosophila* bag-of-marbles protein in the differentiation of cystoblasts from germline stem cells. *Development*. 121:2937–2947.

Micchelli, C.A., and N. Perrimon. 2006. Evidence that stem cells reside in the adult *Drosophila* midgut epithelium. *Nature*. 439:475–479. http://dx.doi.org/10.1038/nature04371

Ohlstein, B., and A. Spradling. 2006. The adult *Drosophila* posterior midgut is maintained by pluripotent stem cells. *Nature*. 439:470–474. http://dx.doi.org/10.1038/nature04333

Ohlstein, B., and A. Spradling. 2007. Multipotent *Drosophila* intestinal stem cells specify daughter cell fates by differential notch signaling. *Science*. 315:988–992. http://dx.doi.org/10.1126/science.1136606

Okada, K., C. Wangpoengtrakul, T. Osawa, S. Toyokuni, K. Tanaka, and K. Uchida. 1999. 4-Hydroxy-2-nonenal-mediated impairment of intracellular proteolysis during oxidative stress. Identification of proteasomes as target molecules. *J. Biol. Chem.* 274:23787–23793. http://dx.doi.org/10.1074/jbc.274.34.23787

Parmentier, M.L., D. Woods, S. Greig, P.G. Phan, A. Radovic, P. Bryant, and C.J. O'Kane. 2000. Rapsynoid/partner of inscuteable controls asymmetric division of larval neuroblasts in *Drosophila*. *J. Neurosci.* 20:RC84.

Rujano, M.A., F. Bosveld, F.A. Salomons, F. Dijk, M.A. van Waarde, J.J. van der Want, R.A. de Vos, E.R. Brunt, O.C. Sibon, and H.H. Kampinga. 2006. Polarised asymmetric inheritance of accumulated protein damage in higher eukaryotes. *PLoS Biol.* 4:e417. http://dx.doi.org/10.1371/journal.pbio.0040417

Shcheprova, Z., S. Baldi, S.B. Frei, G. Gonnet, and Y. Barral. 2008. A mechanism for asymmetric segregation of age during yeast budding. *Nature*. 454:728–734.

Shellenbarger, D.L., and J.D. Mohler. 1975. Temperature-sensitive mutations of the notch locus in *Drosophila melanogaster*. *Genetics*. 81:143–162.

Siller, K.H., C. Cabernard, and C.Q. Doe. 2006. The NuMA-related Mud protein binds Pins and regulates spindle orientation in *Drosophila* neuroblasts. *Nat. Cell Biol.* 8:594–600. http://dx.doi.org/10.1038/ncb1412

Song, X., C.-H. Zhu, C. Doan, and T. Xie. 2002. Germline stem cells anchored by adherens junctions in the *Drosophila* ovary niches. *Science*. 296:1855–1857. http://dx.doi.org/10.1126/science.1069871

Toroser, D., W.C. Orr, and R.S. Sohal. 2007. Carbonylation of mitochondrial proteins in *Drosophila melanogaster* during aging. *Biochem. Biophys. Res. Commun.* 363:418–424. http://dx.doi.org/10.1016/j.bbrc.2007.08.193

Vernace, V.A., T. Schmidt-Glenewinkel, and M.E. Figueiredo-Pereira. 2007. Aging and regulated protein degradation: who has the UPPer hand? *Aging Cell*. 6:599–606. http://dx.doi.org/10.1111/j.1474-9726.2007.00329.x

Wang, Y., A.B. Meriin, N. Zaarur, N.V. Romanova, Y.O. Chernoff, C.E. Costello, and M.Y. Sherman. 2009. Abnormal proteins can form aggresome in yeast: aggresome-targeting signals and components of the machinery. *FASEB J.* 23:451–463. http://dx.doi.org/10.1096/fj.08-117614